Amplification of fluorescence using collinear picosecond optical parametric amplification at degeneracy*

Zhang Jing(张 静)[a)], Zhang Qiu-Lin(张秋琳)[a)], Jiang Man(江 曼)[a)], Zhang Dong-Xiang(张东香)[a)], Feng Bao-Hua(冯宝华)[a)†], and Zhang Jing-Yuan(张景园)[b)]

[a)] *Beijing National Laboratory for Condensed Matter Physics, Institute of Physics, Chinese Academy of Sciences, Beijing* 100190, *China*

[b)] *Department of Physics, Georgia Southern University, Statesboro, GA* 30460, *USA*

(Received 27 February 2012; revised manuscript received 21 March 2012)

We demonstrate the output characteristic of broadband parametric amplification of incoherent light pulses in a 355-nm pumped degenerate picosecond optical parametric amplification with either saturated or unsaturated amplification. The optical parametric amplifier is seeded by the fluorescence generated in a solution of pyridine-1 dye in ethanol. With the saturated amplification, we can obtain high energy incoherent light pulses, whose full width at half maximum bandwidth varies from 16 nm to 53 nm for the different phase matching angles near degeneracy. Moreover, the unsaturated bandwidth of the amplified pulses fits well to the calculated result at degeneracy. Selecting s-polarized fluorescence with a Glan–Taylor prism, the maximum bandwidth of the amplified fluorescence is found to be 59 nm for a purely s-polarized seed. The maximum output energy is 0.67 mJ for the optical parametric amplifier. By using an optical filter and compressor, the generated high energy incoherent light has great potential as the incoherent pump, signal or idler wave of a parametric down-conversion process, so that a wave with a high degree of coherence can be generated from an incoherent pump light.

Keywords: broadband parametric amplification, fluorescence, degeneracy, picosecond optical parametric amplifier

PACS: 42.65.Yj, 42.65.Ky, 32.50.+d, 42.65.Re **DOI:** 10.1088/1674-1056/21/8/084211

1. Introduction

Optical parametric amplification (OPA) is a second-order nonlinear process, and is related to the interaction of three waves, namely, the pump, the signal, and the idler. Both energy conservation and momentum conservation are required to be satisfied when a shorter-wavelength pump wave is down-converted into a signal and an idler wave simultaneously.[1] In the meantime, the OPA can provide broad gain bandwidth and extremely high gain when an optical signal is injected into OPA at either idler or signal wavelength under suitable phase matching condition. During the past two decades, OPA has become an important tool for the generation of broadband optical laser pulses with high energy. Broad gain bandwidth in an OPA is achieved when the group velocities of the signal and the idler are matched. There are two types of geometries to satisfy the condition, namely, collinear and noncollinear geometry. For collinear geometry, a broadband OPA can be realized at degeneracy in type I phase matching configuration due to the equal frequencies of the signal and idler waves. Recently, Siddiqui *et al.*[2] reported on the generation of ultra-broadband pulses at 800 nm from a degenerate OPA seeded by a white light continuum. For a noncollinear geometry, a broadband OPA is operated away from degeneracy, in which the signal group velocity equals the projection of the idler group velocity along the signal direction. It the most common that the second harmonic of Ti:sapphire laser pumped noncollinear beta barium borate (BBO)-OPA in the visible region.[3−5] Using these concepts, a variety of broadband OPA schemes, seeded by broadband coherent light pulses, have been demonstrated.[2−9]

In the recent years, using OPA as an amplifier for ultra-weak coherent and incoherent signals has gained considerable research interest. Although the broadband parametric amplification of fluorescence based on noncollinear OPA[10−13] has been reported, their

*Project supported by the National Basic Research Program of China (Grant No. 2007CB613205) and the National Natural Science Foundation of China (Grant No. 61078005).

†Corresponding author. E-mail: bhfeng@aphy.iphy.ac.cn

© 2012 Chinese Physical Society and IOP Publishing Ltd

main research purpose is to use the broadband OPA to study the dynamics of fluorescence with a femtosecond time-resolution or to find the detection limit of the OPA. The femtosecond-OPA provides femtosecond time-resolved analysis, however, the lifetime of most of the fluorescence is on the nanosecond scale. A picosecond OPA is well suitable for the study of fluorescence. In a type-I phase-matched collinear OPA, the bandwidth is much broader at degeneracy than that at other wavelength for a nonlinear crystal due to its much larger angular dispersion ($\mathrm{d}\lambda/\mathrm{d}\theta$) at degeneracy. Therefore, the picosecond collinear OPA working at degeneracy is particularly useful for the amplification of fluorescence, whose spectral range overlaps with the wavelength range of the gain spectra of the OPA at degeneracy. Even more importantly, broadband incoherent light pulses with high energy can be obtained from the OPA seeded by fluorescence. Under certain conditions, a coherent signal can be generated from an incoherent pump light in parametric down-conversion process.[14,15] Hence by using an optical filter and a compressor, the generated high energy incoherent light can be used as an incoherent pump, signal or idler wave of a down-conversion process. However, the output characteristic of the broadband parametric amplification of incoherent light pulses based on picosecond collinear OPA at degeneracy with either saturated or unsaturated amplification has not been investigated.

In this paper, we demonstrate the output characteristic of broadband parametric amplification of the fluorescence generated in a solution of pyridine-1 dye in ethanol using a 355-nm pumped picosecond collinear type-I phase-matched OPA. The spectral range of the gain of the OPA near degeneracy partially overlaps with the fluorescence spectrum (from 594 nm to 803 nm). For the OPA near degeneracy with saturated amplification, we can obtain high-energy incoherent light pulses with full width at half maximum (FWHM) bandwidth varying from 16 nm to 53 nm. Moreover, when the OPA is not saturated, the FWHM bandwidth of the amplified pulses fits well to the calculated result at degeneracy. Furthermore, selecting the fluorescence by a Glan–Taylor prism, broadband amplification with an FWHM bandwidth of 59 nm is achieved for a purely s-polarized seed. Such a difference is attributed to additional angular dispersion introduced by the prism. At a phase matching angle of 33.16°, the maximum output energy is 0.67 mJ in the OPA stage.

2. Experimental setup

Our collinear OPA experimental setup is shown in Fig. 1. The single stage parametric amplifier, with a design similar to that reported in Ref. [16] starts with a 10-Hz passively/actively mode-locked Nd:YAG laser (EKSPLA:PL2143B). It employs an 11-mm-thick BBO crystal cut for type I phase-matching ($\theta_{\mathrm{c}} = 28.5°$, $\phi_{\mathrm{c}} = 0°$), pumped by the third harmonic of the Nd:YAG laser (355 nm, p-polarized, 15 ps) and seeded by the fluorescence generated in a solution of pyridine-1 dye in ethanol with a concentration of 4×10^{-3} M/L. The dye solution is excited by the second harmonic pulse (532 nm, s-polarized, 18 ps) of 35 μJ, which is focused with an $f = 50$ mm lens (L1) into a 5-mm-thick quartz sample cell. The spectral range of the fluorescence covers from 598 nm to 778 nm measured by a spectrometer after the sample cell. At the input face of the BBO crystal, the seed and the pump beams are collimated to a diameter of roughly 2.25 mm by an $f = 100$ mm lens (L2) and 3.3 mm by a telescope (TS), respectively. The temporal and spatial overlap between the pump and the seed in the BBO crystal are achieved through a delay stage in the pump arm and a dichroic mirror M6, respectively. The energy of the amplified pulses is detected with an energy meter. The amplified pulses are spectrally analysed with a CCD-spectrometer (Ocean Optics, HR2000).

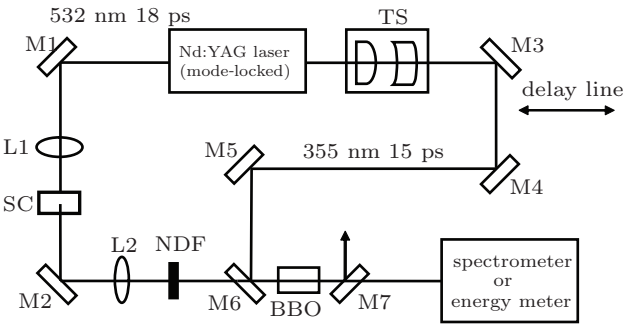


Fig. 1. Schematic diagram of the experimental arrangement: TS: telescope; M1: mirror (highly reflective at 532 nm); L1–L2: lenses; SC: sample cell; M2: silver mirror; NDF: neutral density-filters; M3–M7: mirrors (highly reflective at 355 nm).

3. Results and discussion

The intensity gain of the amplified signal beam can be obtained from the analytical solution of the coupled-wave equations in the slowly varying envelope approximation, under the assumption of no significant

pump depletion and neglecting the group-velocity mismatching. The intensity gain G equation was given in Ref. [17]. The gain spectra for BBO crystal can be calculated based on the intensity gain equation[17] and the revised Sellmeier equations of BBO crystal.[18] Figure 2(a) displays the simulation results of the normalized parametric gain spectra of BBO at degeneracy and near degeneracy in type-I phase-matched collinear configuration. The parameters of the simulation are adapted to the experiment described below, i.e., 11-mm-long length BBO crystal, 355-nm pump wavelength and 1.52 GW/cm^2 pump intensity. The simulated results show that when the phase matching condition is slightly detuned from the degeneracy, it results in the generation of a broad double humped spectrum so that the parametrically generated radiation has a slightly broader gain bandwidth.[2] In other words, the gain bandwidth near degeneracy ($\theta = 33.17°, 33.175°$) is larger than that at degeneracy ($\theta = 33.18°$), because the phase-matching is simultaneously achieved at two wavelengths and the signal pulses travel with group velocities very close to that of the idler near degeneracy. When the phase matching angle is about 33.175°, which is slightly off the degeneracy, the FWHM gain bandwidth is about 48 nm covering a spectral range from 675 nm to 748 nm. Moreover, the FWHM bandwidth is reduced to 40 nm at degeneracy in a range from 678 nm to 745 nm. Moreover, when the crystal angle is rotated away from the phase matching angle at or near degeneracy, the phase matching is satisfied at two separated wavelengths. The corresponding gain bandwidth is small compared with that at degeneracy or near degeneracy.[19]

Firstly, we check the polarization of the generated fluorescence by using a linear polarizer located behind the Glan–Taylor prism as analyser and by measuring the full spectrum through the analyser. The Glan–Taylor prism is placed in front of the dichroic mirror M6. The measured extinction ratio of the seed is $> 10^3$:1 after the Glan–Taylor prism. We also measure the seed energy behind the Glan–Taylor prism with an energy meter. The s-polarized seed energy is 60 nJ, which is smaller than the seed energy of 73 nJ in front of the Glan–Taylor prism. Then the Glan–Taylor prism is rotated by 90° degrees and the transmitted p-polarized seed energy is 8.2 nJ. This means that for an s-polarized excitation beam at 532 nm the generated fluorescence is mainly s-polarized along the polarization of the excitation pulse with an ellipticity ratio $\rho = I_s/I_p \sim 7.32$.

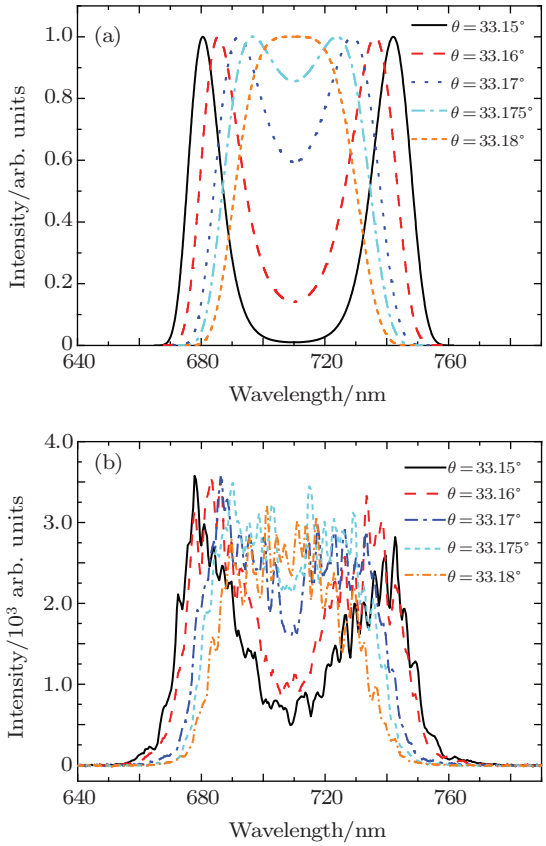


Fig. 2. (colour online) (a) Calculated parametric gain spectra of BBO crystal at degeneracy and near degeneracy. The gain is normalized to the peak value at degeneracy. (b) Amplified spectra of the 355-nm pumped OPA at degeneracy and near degeneracy in the case of saturated amplification.

Secondly, the generated fluorescence is directly amplified in the degenerate BBO–OPA without polarization selection with a Glan–Taylor prism. The pump energy and the seed energy in front of the used BBO crystal are 1.95 mJ and 73 nJ, respectively. The amplified spectra at degeneracy and near degeneracy (approximately $\theta = 33.15°, 33.16°, 33.17°, 33.175°$) are presented in Fig. 2(b). Based on the revised Sellmeier equations of BBO crystal,[18] the phase matching angles are calculated by the corresponding optical parametric super-fluorescence spectral profile, with an excitation source at 532 nm blocked. It can be seen from Fig. 2(b) that with the crystal angle tuned gradually toward a phase matching angle of 33.18° at degeneracy, the two peaks near degeneracy become closer and finally combine into a single peak. The FWHM bandwidth of the amplified pulses varies from 16 nm to 53 nm for the different phase matching angles near degeneracy. When the phase-matching angle is at 33.175°, the maximum broadband pulse of 53 nm at

the FWHM bandwidth is obtained, whose wavelength is in a range from 665 nm to 754 nm. The difference between the calculation and the experimental results can be attributed mainly to saturated amplification in the OPA stage and the spectral profile of the generated fluorescence. The FWHM bandwidth of the amplified pulses is 39 nm at degeneracy, which is small compared with that near degeneracy ($\theta = 33.175°$). Although the FWHM bandwidth of the amplified pulses fits well to the calculated result at degeneracy, its wavelength range (from 669 nm to 751 nm) is different from the simulated result.

We attenuate the seed energy with neutral-density-filters (NDF) to make sure that there is no gain saturation in the OPA at the seed level used in our work. Considering the attenuation factor of the NDF and the generated fluorescence energy of 73 nJ, the seed energy is on the order of femto-joule. In our previous work,[20] we reported on for the tens of femto-joule seed, the amplification is linear and no gain saturation occurs in the OPA. Figure 3 presents the amplified spectra for the tens of femto-joule level seed at degeneracy and near degeneracy (approximately $\theta = 33.15°$, $33.16°$, $33.17°$, $33.175°$). The FWHM bandwidth of the amplified pulses is 39 nm at degeneracy, whose wavelength ranges from 678 nm to 745 nm. It basically accords with the calculated results. For the tens of femto-joule level seed, the wavelength region of the amplified spectrum near degeneracy is also in agreement with the calculated results. However, the FWHM bandwidth of the amplified pulses near degeneracy is small compared with simulated results presumably due to the spectral distribution of the seed and the slightly different attenuation factor for different wavelengths.

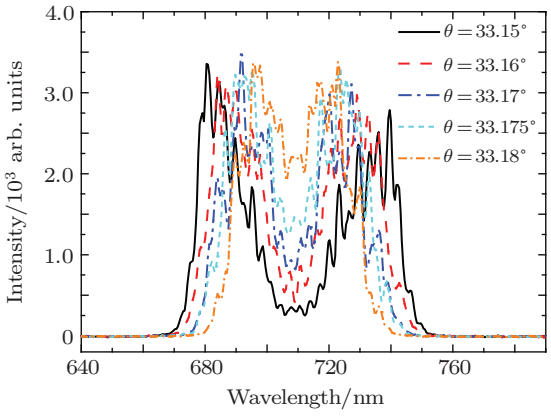


Fig. 3. (colour online) Amplified spectra of the 355-nm pumped OPA at degeneracy and near degeneracy for the femto-joule level seed.

When the parametric amplification is saturated, a photograph of the typically amplified beam pattern at the phase matching angle of 33.15° is shown in Fig. 4(a) and, for comparison, figure 4(b) illustrates the photograph of the corresponding optical parametric super-fluorescence, with the excitation source at 532 nm blocked, so that the OPA is not seeded. From Fig. 4, it is clearly observed that the presence of the seed not only receives a huge gain from the pump, but also takes over the parametric gain of super-fluorescence as can be seen from the much weaker super-fluorescence when the OPA is seeded.

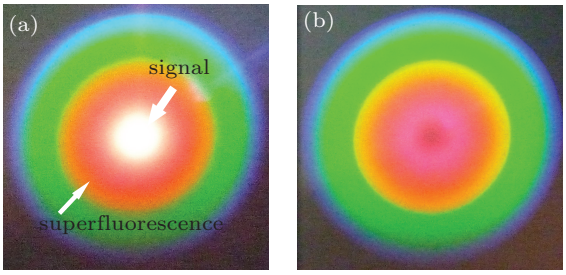


Fig. 4. (colour online) (a) Photograph of the amplified fluorescence with an optical parametric super-fluorescence beam pattern at the phase matching angle of 33.15°; (b) photograph of the corresponding optical parametric super-fluorescence without seeding in the OPA. They are recorded by using a common CCD camera.

We then examine the polarization dependence of the OPA by selecting the generated fluorescence using a Glan–Taylor prism placed in front of the dichroic mirror M6. At the maximum transmittance of the Glan–Taylor prism, the fluorescence is purely s-polarization after passing through the prism, which corresponds to an o-wave in the OPA. As previously mentioned, when the Glan-prism is removed, the seed is elliptically polarized with about 11% of the seed that is p-polarized. It is expected that the p-polarized fluorescence is an e-wave in the OPA and it cannot be amplified in a type-I OPA, so that there should be no spectral difference between the polarization-selected case and no polarization-selected case. The amplified spectrum of the purely s-polarized seed at the phase matching angle of 33.175° is shown as a solid curve in Fig. 5: it spans from 660 nm to 760 nm. The amplified spectrum of the elliptically polarized seed is also presented under the same phase matching angle condition with a red dashed curve in Fig. 5. To our surprise, the FWHM bandwidth for the purely s-polarized seed is 59 nm and it is broader than that of elliptically polarized seed as can be observed from Fig. 5. The slightly broadening in the bandwidth of s-polarized

seeding can be attributed to the additional angular dispersion of the fluorescence in the principal plane of the used BBO crystal through the Glan–Taylor prism. Consequently, the phase matching in the OPA is satisfied not only for the central wavelength of signal wave, but also simultaneously for noncollinear components at slightly different wavelengths so that the gain bandwidth is broadened.[21] This is similar to the enhancement caused by adding angular dispersion to the pump.[6] Furthermore, the additional broadening can also be related to the dispersion characteristic, the structure parameters and the angle of incidence in the Glan–Taylor prism.

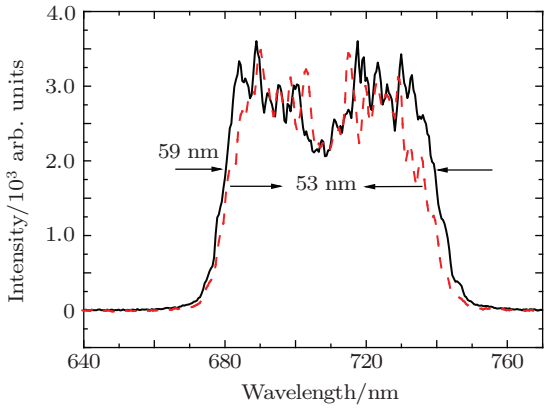


Fig. 5. (colour online) Amplified spectra with maximal FWHM bandwidth in the case of the elliptically polarized seed (red dashed curve) and the s-polarized seed (black solid curve).

Finally, we measure the output energies at the different phase matching angles in the OPA stage as shown in Table 1. The pump energy and the seed energy are 1.95 mJ and 73 nJ, respectively. At the phase matching angle of 33.16°, the maximum output energy decreases from 0.67 mJ for the elliptical polarization seed to 0.65 mJ for the s-polarized seed due to the insertion loss of the prism. The p-polarized component of the fluorescence or e-wave seeding in the OPA cannot be amplified in a type-I OPA. The output energy can be increased by cascading OPA or increasing the excitation energy at 532 nm.

Table 1. Output energies at the different phase matching angles in the OPA stage. (e and s mean the OPAs injected by elliptically polarized seed and s-polarized seed, respectively. The seed energies of elliptically polarized seed and s-polarized seed are 73 nJ and 60 nJ, respectively.)

Phase matching angle/(°)	Output energy/mJ$^{\rm e}$	Output energy/mJ$^{\rm s}$
33.15	0.64	0.61
33.16	0.67	0.65
33.17	0.61	0.59
33.175	0.57	0.55
33.18	0.49	0.47

4. Conclusion

In this paper, we demonstrate the broadband parametric amplification of incoherent light pulses in a degenerate picosecond type-I BBO-OPA. The OPA is pumped by the third harmonic of Nd:YAG laser at 355 nm and seeded by the fluorescence generated by a solution of pyridine-1 dye in ethanol. The wavelength range of gain spectra of the OPA near degeneracy partially overlaps with the fluorescence spectrum (from 594 nm to 803 nm). In the case of saturated amplification, we obtain high-energy incoherent pulses with FWHM bandwidth varying from 16 nm to 53 nm for the OPA seeded by generated fluorescence. When the OPA is not saturated by attenuating the seeder energy with neutral density filters, the FWHM bandwidth of the amplified pulses is in accordance with the calculated result at degeneracy. Selecting the s-polarized generated fluorescence by a Glan–Taylor prism, a broadband amplification with an FWHM bandwidth of 59 nm is achieved due to additional angular dispersion introduced by the prism. At the phase matching angle of 33.16°, the maximum output energy is 0.67 mJ for the OPA seeded by the generated fluorescence. The output energy can be increased by cascading OPA or increasing the excitation energy at 532 nm. By using optical filter and compressor, the generated high-energy incoherent light has a great potential as the incoherent pump, signal or idler wave of a parametric down-conversion process.

References

[1] Baumgartner R A and Byer R L 1979 *IEEE J. Quantum Electron.* **15** 432

[2] Siddiqui A M, Cirmi G, Brida D, Kärtner F X and Cerullo G 2009 *Opt. Lett.* **34** 3592

[3] Wilhelm T, Piel J and Riedle E 1997 *Opt. Lett.* **22** 1494

[4] Cerullo G, Nisoli M and De Silvestri S 1997 *Appl. Phys. Lett.* **71** 3616

[5] Shirakawa A, Sakane I and Kobayashi T 1998 *Opt. Lett.* **23** 1292

[6] Limpert J, Aguergaray C, Montant S, Manek-Hönniger I, Petit S, Descamps D, Cormier E and Salin F 2005 *Opt. Express* **13** 7386

[7] Zhao B Z, Liang X Y, Leng Y X, Jiang Y L, Wang C, Lu H H, Du J, Xu Z Z and Shen D Z 2006 *Appl. Opt.* **45** 565

[8] Khakhulin D V, Savel'ev A B and Volkov R V 2007 *Laser Phys. Lett.* **4** 345

[9] Cirmi G, Brida D, Manzoni C, Marangoni M, De Silvestri S and Cerullo G 2007 *Opt. Lett.* **32** 2396

[10] Fita P, Stepanenko Y and Radzewicz C 2005 *Appl. Phys. Lett.* **86** 021909

[11] Chen X H, Han X F, Weng Y X and Zhang J Y 2006 *Appl. Phys. Lett.* **89** 061127

[12] Han X F, Chen X H, Weng Y X and Zhang J Y 2007 *J. Opt. Soc. Am.* B **24** 1633

[13] Han X F, Weng Y X, Pan A L, Zou B S and Zhang J Y 2008 *Appl. Phys. Lett.* **92** 032102

[14] Picozzi A and Haelterman M 2001 *Phys. Rev. Lett.* **86** 2010

[15] Piskarskas A, Pyragaite V and Stabinis A 2010 *Phys. Rev.* A **82** 053817

[16] Zhang J, Zhang Q L, Zhang D X, Feng B H and Zhang J Y 2010 *Appl. Opt.* **49** 6645

[17] Ross I N, Matousek P, Towrie M, Langley A J and Collier J L 1997 *Opt. Commun.* **144** 125

[18] Zhang D X, Kong Y F and Zhang J Y 2000 *Opt. Commun.* **184** 485

[19] Lu Z G, Liu H J, Jing F, Zhao W, Wang Y S and Peng Z T 2009 *Acta Phys. Sin.* **58** 4689 (in Chinese)

[20] Du S F, Zhang D X, Shi Y X, Li Q N, Feng B H, Han X F, Weng Y X and Zhang J Y 2009 *Opt. Commun.* **282** 1884

[21] Piskarskas A P, Stabinis A P and Pyragaite V 2010 *IEEE J. Quantum Electron.* **46** 1031